The Astrophysical Journal, 759:60 (9pp), 2012 November 1 doi:10.1088/0004-637X/759/1/60

WISE J163940.83−684738.6: A Y DWARF IDENTIFIED BY METHANE IMAGING*

C. G. Tinney[1], Jacqueline K. Faherty[2], J. Davy Kirkpatrick[3], Edward L. Wright[4], Christopher R. Gelino[3], Michael C. Cushing[5], Roger L. Griffith[3], and Graeme Salter[1]
[1] Department of Astrophysics, School of Physics, University of New South Wales, Sydney, NSW 2052, Australia; c.tinney@unsw.edu.au
[2] Department of Astronomy, University of Chile, Camino El Observatorio 1515, Casilla 36-D, Santiago, Chile
[3] Infrared Processing and Analysis Center, MS 100-22, California Institute of Technology, Pasadena, CA 91125, USA
[4] Department of Physics and Astronomy, UCLA, Los Angeles, CA 90095-1547, USA
[5] Department of Physics and Astronomy, MS 111, University of Toledo, 2801 W. Bancroft St., Toledo, OH 43606-3328, USA
Received 2012 August 28; accepted 2012 September 19; published 2012 October 17

ABSTRACT

We have used methane imaging techniques to identify the near-infrared counterpart of the bright *Wide-field Infrared Survey Explorer* (*WISE*) source WISE J163940.83−684738.6. The large proper motion of this source ($\approx 3\farcs0\ \mathrm{yr}^{-1}$) has moved it, since its original *WISE* identification, very close to a much brighter background star—it currently lies within $1\farcs5$ of the $J = 14.90 \pm 0.04$ star 2MASS 16394085−6847446. Observations in good seeing conditions using methane-sensitive filters in the near-infrared J band with the FourStar instrument on the Magellan 6.5 m Baade telescope, however, have enabled us to detect a near-infrared counterpart. We have defined a photometric system for use with the FourStar $J2$ and $J3$ filters, and this photometry indicates strong methane absorption, which unequivocally identifies it as the source of the *WISE* flux. Using these imaging observations we were then able to steer this object down the slit of the Folded-port Infrared Echellette spectrograph on a night of $0\farcs6$ seeing, and so obtain near-infrared spectroscopy confirming a Y0–Y0.5 spectral type. This is in line with the object's near-infrared-to-*WISE* $J3 - W2$ color. Preliminary astrometry using both *WISE* and FourStar data indicates a distance of 5.0 ± 0.5 pc and a substantial tangential velocity of $73 \pm 8\ \mathrm{km\ s}^{-1}$. WISE J163940.83−684738.6 is the brightest confirmed Y dwarf in the *WISE* $W2$ passband and its distance measurement places it among the lowest luminosity sources detected to date.

Key words: brown dwarfs – methods: observational – parallaxes – stars: individual (WISE J163940.83−684738.6) – techniques: photometric

Online-only material: color figures

1. INTRODUCTION

Data from the NASA *Wide-field Infrared Survey Explorer* (*WISE*; Wright et al. 2010) have delivered unprecedented advances in our understanding of the properties and space densities of the coldest compact astrophysical sources identified outside our solar system—the Y-type brown dwarfs (Cushing et al. 2011; Kirkpatrick et al. 2012).

These very cold brown dwarfs have scientific impacts that span multiple astronomical arenas. In the field of star formation, they can deliver a historical record of the star formation process at very low masses and at epochs billions of years prior to the star-forming regions we observe today. In the field of planetary atmospheric theory, they represent low-temperature atmospheres that can be readily observed without the contaminating glare of a host star, and without the photochemical complications introduced by host star irradiation. While in the field of exoplanet searches, they provide nearby, low-luminosity search targets potentially hosting planetary systems of their own.

WISE is readily able to identify these very cold brown dwarfs by their mid-infrared methane absorption bands. The shortest wavelength *WISE* band (hereafter $W1$) has a central wavelength of 3.4 μm, which sits in the middle of the strong fundamental methane absorption band near 3.3 μm. The second shortest *WISE* band (hereafter $W2$) has a central wavelength of 4.6 μm, where the photosphere is reasonably transparent, so it detects flux from deeper, hotter layers in the brown dwarf. As a result, cold brown dwarfs can be identified via their very red $W1 - W2$ color. Thirteen Y dwarfs have been identified and spectroscopically confirmed to date by the WISE Brown Dwarf Science Team (Cushing et al. 2011; Kirkpatrick et al. 2012).

2. OBSERVATIONS OF WISE J163940.83−684738.6

The *WISE* source WISE J163940.83−684738.6 (hereafter W1639) passes all the selection criteria for being a cold Y-type brown dwarf (see Kirkpatrick et al. 2012 for details), but the identification of a near-infrared counterpart to the *WISE* flux has proved difficult. With $W2 = 13.64 \pm 0.05$ and $W1 - W2 > 4.24$, W1639 would represent (if confirmed as a brown dwarf) the brightest Y dwarf in the *WISE* survey.

We have been carrying out observations of *WISE* sources since early 2012 using the FourStar infrared mosaic camera (Persson et al. 2008) mounted on the 6.5 m Magellan Baade telescope at Las Campanas Observatory, Chile. This program has dual goals: to contribute to the complete identification of all *WISE* sources with $W1 - W2 > 2.0$; and to carry out astrometric measurements of confirmed cold brown dwarfs. The first of these science goals is pursued using the near-infrared methane-sensitive $J2$ and $J3$ filters installed in FourStar. The $J2$ filter (see Figure 1) is centered on a region in which methane absorption produces strong suppression in very cool brown dwarfs, while the $J3$ filter is centered on one of the few opacity holes (at 1.27 μm) in cold brown dwarf photospheres. In this respect they represent J-band analogous of the H-band CH_4s and CH_4l filters used in the methane system of Tinney et al. (2005).

* This paper includes data gathered with the 6.5 m Magellan Telescopes located at Las Campanas Observatory, Chile.

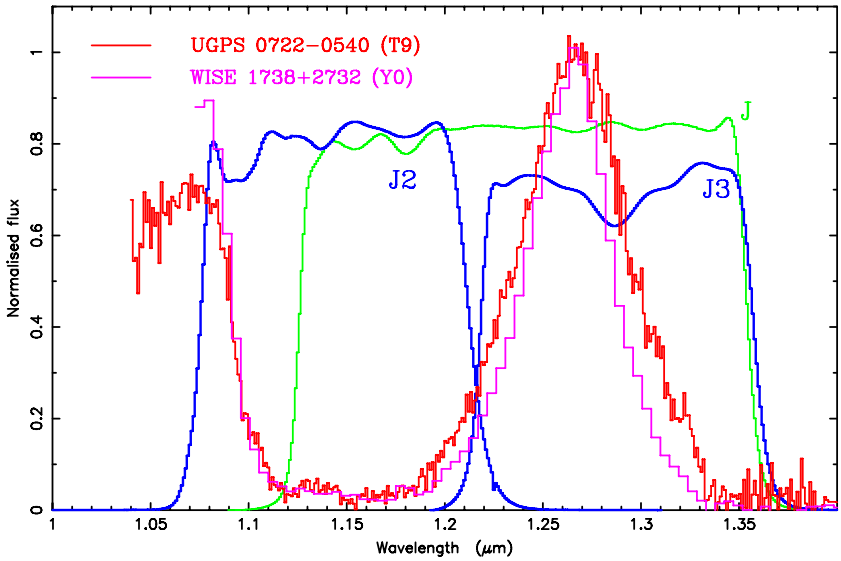

Figure 1. FourStar J, $J2$, and $J3$ filter bandpasses, plotted with example very cool brown dwarf spectra (WISEPA J173835.53+273258.9 from Cushing et al. 2011 and UGPS J072227.51-054031.2 from Lucas et al. 2010—the spectral types are those assigned by Kirkpatrick et al. 2012). The $J3$ filter sees significant flux from brown dwarfs with strong methane absorption, while the $J2$ flux is highly suppressed.

(A color version of this figure is available in the online journal.)

W1639 was observed on 2012 May 10–11 (UT)[6] with FourStar for approximately 4 hr, using 50 exposures of 120 s in each filter and random telescope dithering. Each of FourStar's four 2048 × 2048 pixel detectors sees a field 325″ on a side—in this analysis we deal only with data from a single detector *(Chip2)* in which all our targets were placed. Data processing was performed using a version of the ORACDR pipeline system (Cavanagh et al. 2008)[7] modified by us for use with FourStar. This creates and subtracts averaged dark frames, combines observations of a given target in each filter to create a flat field, flattens all frames and then mosaics them to produce a final image. The results of each first-pass processing with ORACDR were used to identify frames with poor image quality and/or poor transmission, and these were then removed before a second-pass reprocessing. The final images for W1639 are created from the 29 best $J3$ images (totaling 58 minutes of exposure time and delivering 0.″66 images) and the 27 best $J2$ images (totaling 54 minutes and delivering 0.″81 images). The resulting images, centered on W1639's *WISE All Sky* release position, are shown in Figures 2(a) and (b). No obvious source is visible with the very red $J3-J2$ color expected for a cool brown dwarf. The bright source to the south of W1639's position is the $J = 14.90 \pm 0.04$ star 2MASS J163940.85−684744.6 (hereafter 2M1639).

These images were then photometered using the DAOPHOT II package (Stetson 1987), as implemented within the Starlink environment (Draper et al. 2005).[8] Unsaturated point-spread function (PSF) stars were selected within a 1′ radius of W1639, and used to create an initial model PSF. This was used to fit and subtract all identified stars within the image. In many cases this reveals the presence of companion stars within the halos of PSF stars. Identifying these stars and including them in the PSF analysis on a second pass allowed us to iterate toward an "uncontaminated" PSF, which was then used to fit and subtract the bright star 2M1639. The resulting images "cleaned" of this bright star are shown in Figures 2(c) and (d), and demonstrate the existence of a near-infrared source previously hidden within the halo of 2M1639. Moreover this source is bright in $J3$ and faint in $J2$—precisely the signature expected if the *WISE* W1639 flux is due to a cool brown dwarf.

Subsequently, the same field was re-observed as an astrometric target in the $J3$ filter for around 1 hr in each of the nights 2012 July 10, 11 and August 10. These data are discussed further in Section 5.

3. PHOTOMETRY ON THE $J3/J2$ SYSTEM

We can use imaging data to ask what the $J3 - W2$ colors for W1639 imply for this system. We have used SExtractor (Bertin & Arnouts 1996) to obtain aperture photometry for stellar sources in both the "cleaned" W1639 images (obtained as described above), and for processed images of other late-T and Y dwarfs observed with FourStar as part of our *WISE* follow-up program on the nights of 2012 March 9, May 10, and July 10–11. These uncalibrated photometric catalogs were then position-matched against Two Micron All Sky Survey (2MASS) catalog data in these fields for both astrometric and photometric calibration.

With no pre-existing standards to define a $J2/J3$ photometric system, we are forced to define our own system (as we did in Tinney et al. 2005). Following that example, we base our system on Mauna Kea Observatories (MKOs) J-band photometry—i.e., we adopt $J_{\rm MKO}$ standards over a narrow color range to define our magnitude zero point for $J3$ and $J2$. We obtain $J_{\rm MKO}$ photometry for stars in each field by converting 2MASS $JHK_{\rm s}$ photometry to the MKO system, for stars in the color ranges where the transformations in the *Explanatory Supplement to the 2MASS All Sky Data Release and Extended Mission Products*[9] are reliable (i.e., in the range $-0.2 < (J - K_{\rm s})_{\rm 2M} < 1.5$ and $-0.2 < (J - H)_{\rm 2M} < 1.1$).

In Tinney et al. (2005) we used relatively hot A-, F-, and G-type dwarf stars to define a CH_4s and CH_4l magnitude system

[6] All dates and times used in this paper are UT dates and times.
[7] See also http://www.oracdr.org/.
[8] See also http://starlink.jach.hawaii.edu/starlink.
[9] http://www.ipac.caltech.edu/2mass/releases/allsky/doc/

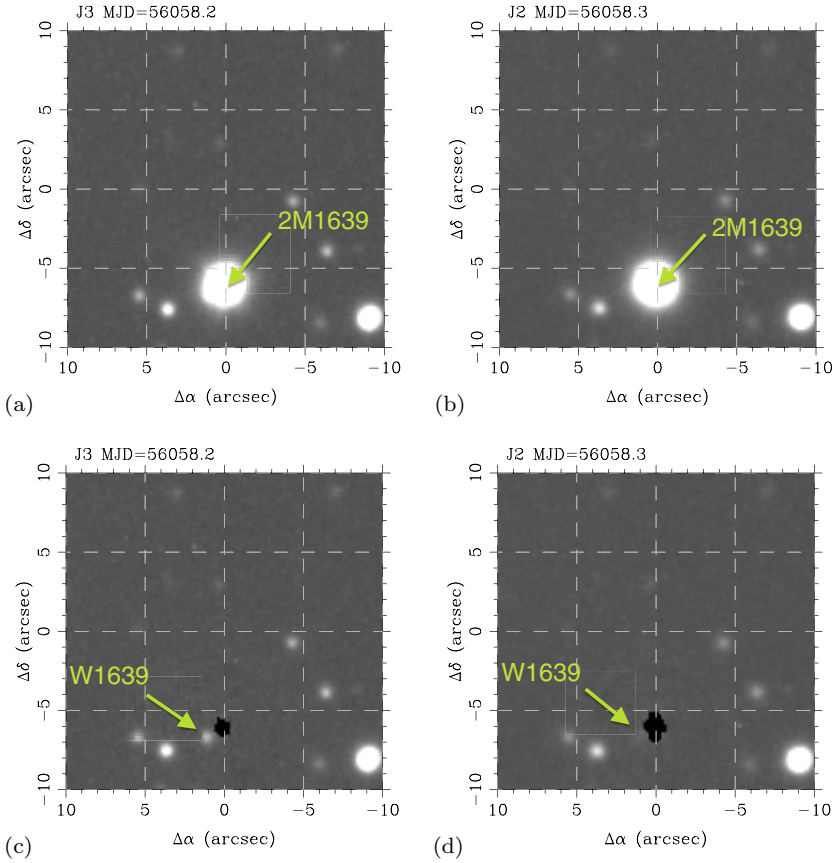

Figure 2. FourStar imaging data centered on the W1639 *WISE All Sky* release position, taken in the $J2$ and $J3$ filters. Panels (a) and (b) show the data from our standard processing, and panels (c) and (d) show the images with the bright source 2M1639 subtracted (as described in the text). The black regions in the lower panels are flagged as bad due to the excess noise arising from imperfect PSF subtraction in 2M1639's core. All panels are plotted with north to the top, and west to the right. (A color version of this figure is available in the online journal.)

in the H band. Unfortunately, such stars (with colors in the range $-0.02 < (J-K)_{\rm MKO} < 0.50$) are rare in an arbitrary FourStar field. Instead we base our $J2/J3$ system on stars in the range $0.4 < (J-K)_{\rm MKO} < 0.8$, corresponding to the spectral type range G6–M3. Fortunately, the color terms involved in the calibration of this $J2$ and $J3$ photometry using $J_{\rm MKO}$ are small. Figure 3 shows a plot of the residuals about this calibration, as a function of $(J-K)_{\rm MKO}$ for more than 400 stars in nine FourStar Chip2 fields—the small dots show individual data points, and the large circles show the results of binning these points into 0.1 mag bins in color, while the dashed line shows a linear fit. There is no evidence for systematic color terms in the residuals for $J2$ over the range $0.0 < (J-K)_{\rm MKO} < 1.3$. The color term present in $J3$ over this range is small ($\approx$0.07 mag mag^{-1}) meaning that using stars with a mean $J-K$ of 0.6, rather than 0.25, would at worst introduce a potential zero-point error of 0.025 mag. This is at a level similar to the standard error in the mean for the zero points obtained in each field, and so neglecting the color term is acceptable.

The result is photometry on the natural system of these $J2$ and $J3$ filters, with a zero point measured using $J_{\rm MKO}$ photometry for stars with $0.4 < (J-K)_{\rm MKO} < 0.8$. This system has the significant advantage that it can deliver high-quality differential $J2/J3$ photometry without the need for absolute photometric conditions. The FourStar field of view typically delivers between 5 and 100 2MASS stars suitable for calibrating each FourStar detector, and typical uncertainties on the determination of this zero point are in the range 0.01–0.02 mag. Table 1 presents photometry on this system for both W1639 and a sample of comparison late-T and Y dwarfs observed with FourStar. Also listed are the relevant *WISE All Sky* release photometry and spectral classifications.

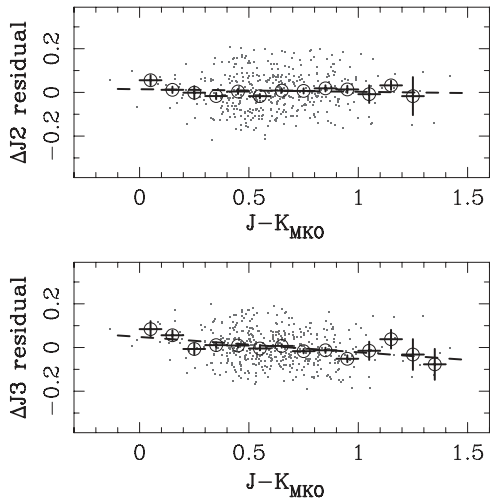

Figure 3. Residuals about $J2$ and $J3$ zero-point calibrations (defined by objects with $0.4 < J-K_{\rm MKO} < 0.8$) as a function of $J-K_{\rm MKO}$. Over 400 stars are plotted as small dots in each panel, representing combined results from nine FourStar fields with one detector. Large circles show the binned means of the dots, while the dashed lines show linear fits to the binned data.

Table 1
FourStar $J3/J2$ Photometry for W1639 and Other *WISE* T and Y Dwarfs

Object	Type	Ref.[a]	J_{MKO}[b]	Obs. Date	$J3$[c]	$J2$	$J3-J2$	$W2$	$J3-W2$
WISEPC J014807.25−720258.7	T9.5	1,5	18.96 0.07	Jul 6	19.83 0.09	20.57 0.10	−0.74 0.14	14.69 0.05	5.14 0.13
WISE J053516.80−750024.9	⩾Y1:	1	...	Mar 9	21.98 0.13	...	...	15.06 0.07	6.92 0.15
WISE J071322.55−291751.9	Y0	1	19.64 0.15	Mar 9	19.48 0.03	21.00 0.05	−1.52 0.06	14.48 0.06	5.00 0.07
WISE J073444.02−715744.0	Y0	1	20.41 0.27	Mar 9	20.06 0.04	...	...	15.36 0.06	4.70 0.07
WISE J081117.81−805141.3	T9.5	2	...	Mar 9, May 10	19.32 0.03 (2)	21.04 0.09	−1.72 0.10	14.38 0.04	4.95 0.05
WISE J091408.96−345941.5	T5	3	...	May 10	17.73 0.02	19.03 0.02	−1.30 0.03	15.03 0.09	2.70 0.09
WISEPC J104245.23−384238.3	T8.5	4	...	Mar 9, May 10, Jul 7	18.57 0.02 (3)	...	...	14.52 0.06	4.05 0.06
WISE J150115.92−400418.4	T6	3	...	May 10	15.95 0.01	17.01 0.01	−1.06 0.02	14.21 0.05	1.74 0.05
WISEPA J154151.66−225025.2	Y0.5	1,6	20.74 0.31	May 10, Jul 7	20.96 0.05 (2)	21.48 0.10[d]	−0.52 0.10[d]	14.25 0.06	6.77 0.09
WISE J163940.86−684744.6	Y0:	6	...	May 10	20.62 0.08	22.27 0.10	−1.65 0.12	13.64 0.05	6.98 0.09
WISE J210200.15−442919.5	T9	3	...	May 10, Jul 6, Jul 7	18.06 0.02 (3)	19.38 0.09	...	14.12 0.05	3.93 0.06
WISEPA J213456.73−713743.6	T9p	1		Jul 6, Jul 7	19.38 0.09	...	...	13.99 0.05	5.39 0.06
WISE J222055.31−362817.4	Y0	1	20.38 0.17	May 10	20.10 0.05 (2)	21.75 0.20	−1.65 0.2	14.66 0.06	5.45 0.09

Notes.
[a] Spectral type sources are: 1, Kirkpatrick et al. (2012); 2, Mace et al. in preparation; 3, C. G. Tinney et al. in preparation; 4, Kirkpatrick et al. (2011); 5, Cushing et al. (2011); 6, this paper.
[b] J_{MKO} values from Kirkpatrick et al. (2012)
[c] Where multiple measures are available, the mean is reported along with the number of observations averaged.
[d] J2 photometry poor due to contaminating $J2 = 18.6$ star 1.″3 away. The real uncertainty will be much larger than the formal photon-counting uncertainty reported here.

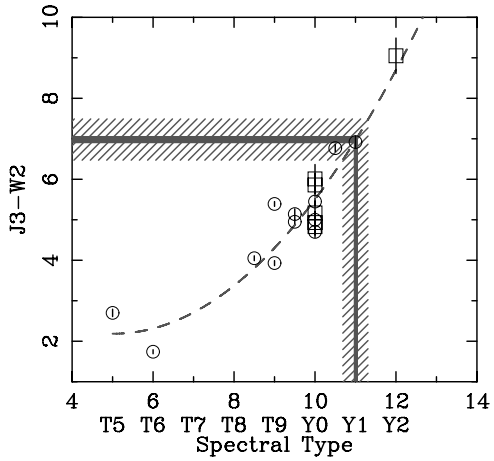

Figure 4. Relationship between $J3-W2$ and spectral type. Circles are the photometry in Table 1, and squares are Y dwarfs with J_{MKO} photometry from Kirkpatrick et al. (2012) converted to $J3$ as described in the text. The dashed line is a quadratic polynomial fit ($J3-W3 = 5.55-1.3428\,n+0.13373341\,n^2$, where n is the numeric parameterization of the T/Y type) with a scatter about the fit of ±0.50 in $J3-W2$. The photometry of W1639 maps it to an equivalent spectral type of Y1 (solid shaded region), while the scatter about the fit (hatched region) maps onto an uncertainty of ±0.3 subtypes.

Figure 4 shows $J3-W2$ colors from Table 1 as a function of spectral type. The Y dwarfs in Table 1 with both J_{MKO} and $J3$ photometry indicate a mean offset between these two systems of $J_{MKO}-J3$=0.14 ± 0.25 for Y dwarfs.[10] Applying this correction to the published J_{MKO} photometry for WISE J173835.53+273259.0, J140518.39+553421.3, J035934.06−540154.6, J041022.71+150248.4, J182831.08+265037.7, and J205628.91+145953.2 in Kirkpatrick et al. (2012) allows us to add computed $J3-W2$ colors and spectral types for these objects (plotted with square symbols) to Figure 4.

[10] Essentially all the Y dwarf flux in the J band emerges within the $J3$ bandpass (see Figure 1), so a simple correction is appropriate—at present most of the scatter in this zero point is due to photon-counting uncertainties for these faint targets.

Much like the plots of $J_{MKO}-W2$ presented in Kirkpatrick et al. (2011), it is clear that $J3-W2$ provides considerable leverage on the measurement of how cool a late-T or Y dwarf is—particularly when combined with a $J3-J2$ color. The latter allows one to determine whether an object has significant methane absorption (i.e., $J3-J2 \lesssim -0.5$), in which case $J3-W2$ can be relied on to be a monotonic estimator of how cool the brown dwarf is (or equivalently of its spectral type). In the case of W1639 (which has almost exactly the same $J3-W2$ as the ⩾Y1: brown dwarf WISE J053516.80+750024.9), this procedure produces a spectral type estimate of Y1 with an uncertainty of ±0.3 subtypes (arising from the scatter about the calibration curve in Figure 4 rather than the precision of the $J3$ photometry).

4. FIRE SPECTROSCOPY

Spectroscopic observations of W1639 were carried out on 2012 July 10 (UT) using the Folded-port Infrared Echellette (FIRE; Simcoe et al. 2008, 2010) on the Magellan Baade telescope. FIRE uses a 2048 × 2048 HAWAII-2RG array and in prism mode delivers a wavelength range from 0.8 to 2.5 μm at a resolution of $\lambda/\Delta\lambda \approx 500$ in the J band (when used with a 0.″6 slit).

Our FourStar astrometric observations on the night of 2012 July 10 were processed on the fly using ORACDR, to obtain a precise position angle and separation at this epoch between the bright source 2M1639 and the faint source W1639. FIRE was rotated to this position angle, and 2M1639 positioned on the slit, ensuring that W1639 would also be acquired down the slit. Six 600 s exposures were obtained nodding the slit by 10″ in an ABBA pattern.

These spectra were then processed in a standard fashion, using arc lines to remove FIRE's optical curvature and traces of the bright star 2M1639 to remove a slight tilt of the spectra with respect to the detector rows. Images were pair subtracted and combined to produce a pair of A–B and B–A images, and these then had any residual sky extracted and subtracted.

The resulting images are dominated by flux from the bright source 2M1639 together with much fainter emission from

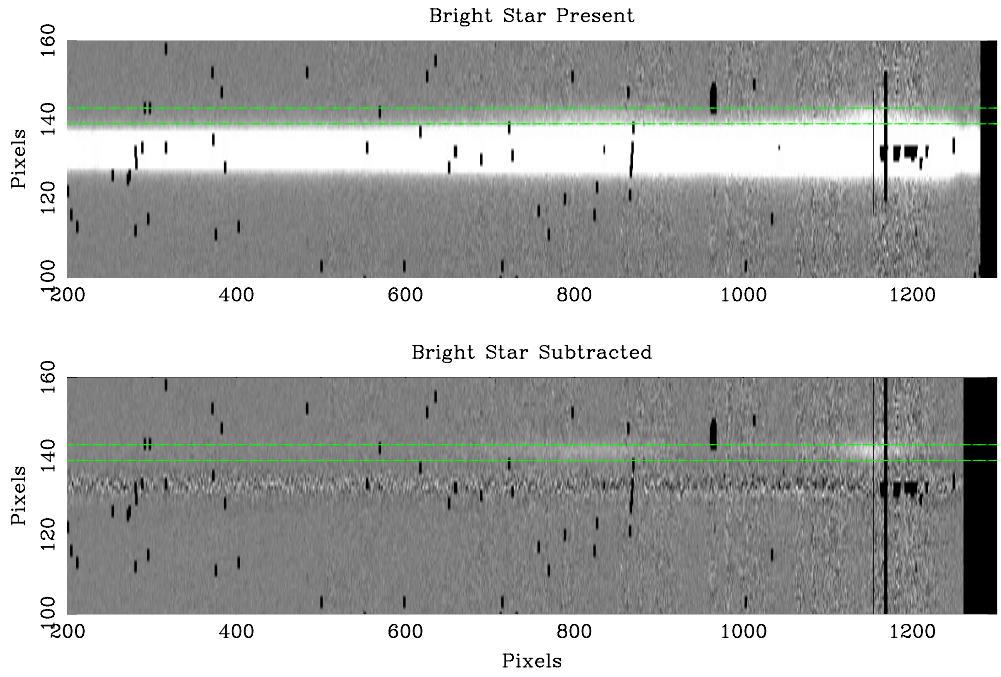

Figure 5. FIRE spectroscopy of 2M1639 and W1639 (upper panel) observed together along the FIRE slit, and (lower panel) after the removal of the signature of 2M1639, using the spatial point-spread function procedure described in the text. The overlaid dashed lines show the location of a 0.″6 wide extraction region centered on the position of W1639. The axes are labeled in FIRE pixel coordinates, after the removal of distortions as described in the text.

(A color version of this figure is available in the online journal.)

W1639 (which is offset by +9.2 pixels in the FIRE data). The expected spectrum of a very late T or Y dwarf can be seen nonetheless in these data (see Figure 5, upper panel). To remove the contaminating flux due to the bright companion, we implemented a "spectral PSF" subtraction using custom scripts in the Perl Data Language.[11] We extracted spatial profiles from the spectra by averaging every 100 pixels in the spectral direction, and fitting a model PSF to the resulting spatial profile—after much experimentation we settled on a Gaussian model for the core of the spectral PSF, a Moffat function for its wings, and we also allowed for a "companion" Gaussian (with the same width as the core) at the spatial separation known between W1639 and 2M1639, but with an amplitude allowed to float as a free parameter. We found that even this model, however, left systematic residuals when subtracted, and so we followed the lead of DAOPHOT (Stetson 1987) and allowed for an empirical look-up table of residuals as a fraction of the total peak height of the spectral PSF. The free parameters for the spectral PSF were then fitted with quadratic polynomials to generate a model PSF that varied smoothly with wavelength. This PSF (minus the "companion" terms that modeled W1639) was then generated, normalized to each column of the image, and subtracted to create a "cleaned" spectral image (see Figure 5, lower panel). Spectra were then extracted from this image, wavelength calibrated and averaged over the A–B and B–A beams to produce a final extracted spectrum (see Figure 6).

Despite the considerable care with which we removed the 5 mag brighter spectrum of 2M1639, Figure 6 indicates that there is nonetheless some contaminating 2M1639 flux still present in the extracted spectrum. This is demonstrated by the flux seen in the extracted spectrum at 1.36–1.4 μm—very cool brown dwarfs emit essentially *zero* flux at these wavelengths, and they *certainly* do not show sharp atmospheric absorption at 1.36 μm. The spectrum of 2M1639 does, however, show such a feature and a scaled version of that spectrum (shown in the figure) is an excellent match to the "baseline" flux present in the extracted spectrum. We are therefore confident that removing the scaled 2M1639 spectrum, as shown, is required to generate a decontaminated spectrum of W1639. This decontaminated spectrum was then binned by a factor of three (to match spectral pixels to the FIRE resolution in this wavelength range) and a telluric star correction applied to remove atmospheric absorption as well as place our spectra on an F_λ scale. The final spectrum is shown in Figure 7.

We then follow the procedure outlined in Kirkpatrick et al. (2012), and rank the relative lateness of W1639 against other Y dwarfs using a comparison of spectra scaled by the flux peak in the *J* band. W1639 is clearly seen to have a *J*-band peak narrower than that of the T9 prototype UGPS 0722, and itself has a *J*-band peak significantly broader than that of the Y1 prototype WISE 0350. It matches best the Y0 prototype, but given the quality of the spectra we have obtained for this difficult-to-observe object, it could lie anywhere in the range Y0–Y0.5.

It is tempting to associate the features seen near 1.03 μm in this spectrum with the NH_3 features near 1.03 μm predicted by the models of Saumon et al. (2012, see their Figure 7). To examine this we plot in Figure 8 the W1639 spectrum near this wavelength before rebinning, along with the 500K BYTe NH_3 model in Saumon et al.'s Figure 7. The alignment of the predicted NH_3 "doublet" feature near 1.02 and 1.035 μm is tantalizing, but due to the noise added to the spectral extraction by the contaminating flux of the bright companion, we are unable to claim this as a robust NH_3 detection from these data alone.

5. ASTROMETRY

W1639 has now been observed at four epochs with Magellan on three observing runs. It was also observed at two epochs

[11] http://pdl.perl.org

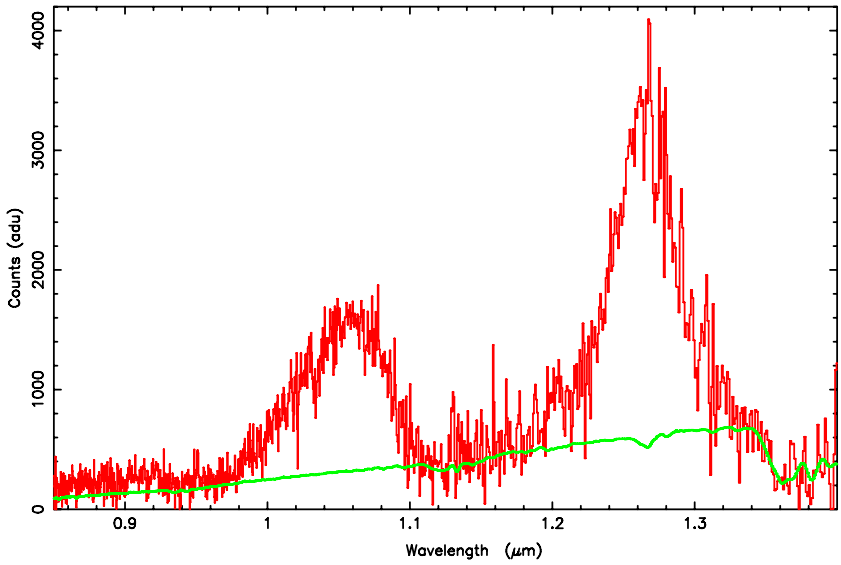

Figure 6. FIRE spectrum of W1639 extracted as described in the text, with a scaled version of the 2M1639 spectrum overplotted to match the flux seen in the contaminated spectrum in the 1.36–1.40 μm range where the flux emitted by a cool brown dwarf will be completely negligible. The vertical scale is in counts per 3600 s.

(A color version of this figure is available in the online journal.)

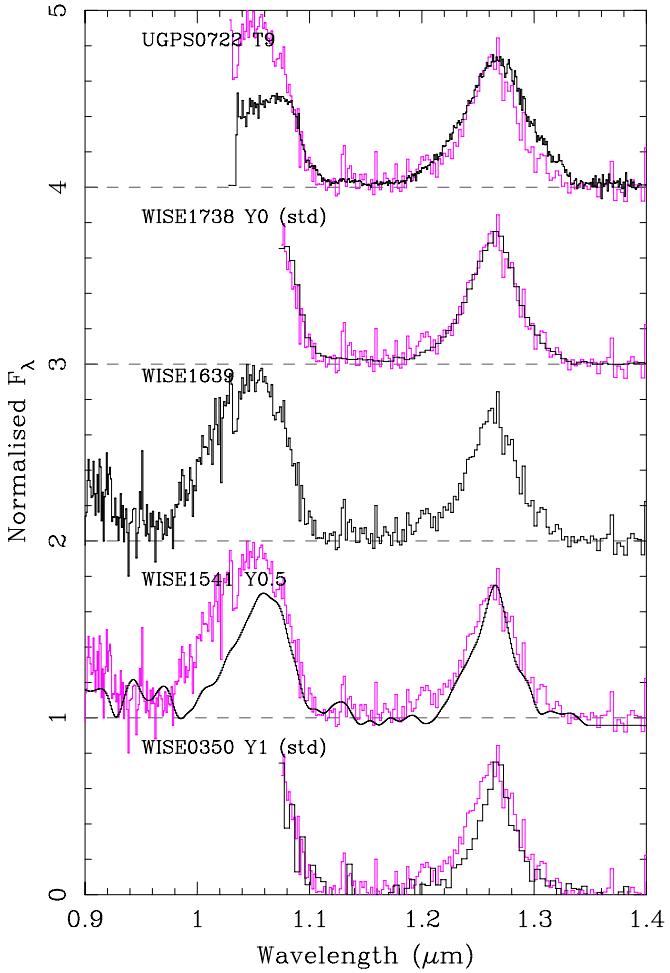

Figure 7. FIRE spectrum of W1639 compared (following Kirkpatrick et al. 2012) with late-T and Y standards. All spectra have been normalized to value 0.75 at the *J*-band peak, and had an arbitrary offset applied for display purposes. The W1639 spectrum is shown in black in the central spectrum, and reproduced in magenta (in online color version) or gray (in published paper version) behind the other spectra.

(A color version of this figure is available in the online journal.)

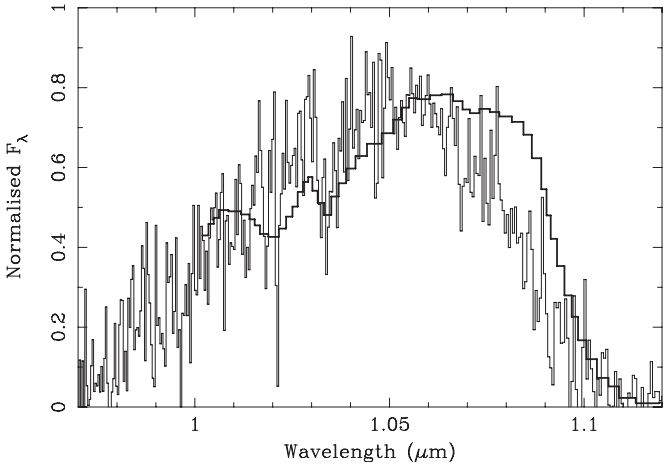

Figure 8. Expanded region of the unbinned spectra in the vicinity of 1.03 μm, along with the 500 K model of Saumon et al. (2012) including opacities due to NH_3 (thick line). The two spectra have been normalized to $F_\lambda = 0.75$ in the range 1.045–1.055 μm.

by *WISE*. Given its very large proper motion, and the fact a Y spectral type and $J3 = 20.62 \pm 0.08$ would suggest a likely distance of less than 10 pc, an astrometric analysis is warranted.

FourStar. Our $J3$ passband, ORACDR-processed images were analyzed using DAOPHOT to obtain precision differential astrometry in a manner identical to that used by us in previous astrometric papers (Tinney et al. 2003; Tinney 1996). We use local 2MASS sources within the FourStar field to determine the plate scale ($0.1592 \pm 0.''0001$ pixel^{-1}) and the orientation to the cardinal directions of a single frame, which is selected for use as an astrometric master.

WISE. W1639 was observed twice by *WISE*—once as part of the *WISE All Sky* release and once again as part of the *WISE 3 Band Cryo* extended mission. We have extracted data from both these catalogs in a 600″ region around W1639 using the Infrared Science Archive gateway.[12] The reported photometry

[12] http://irsa.ipac.caltech.edu

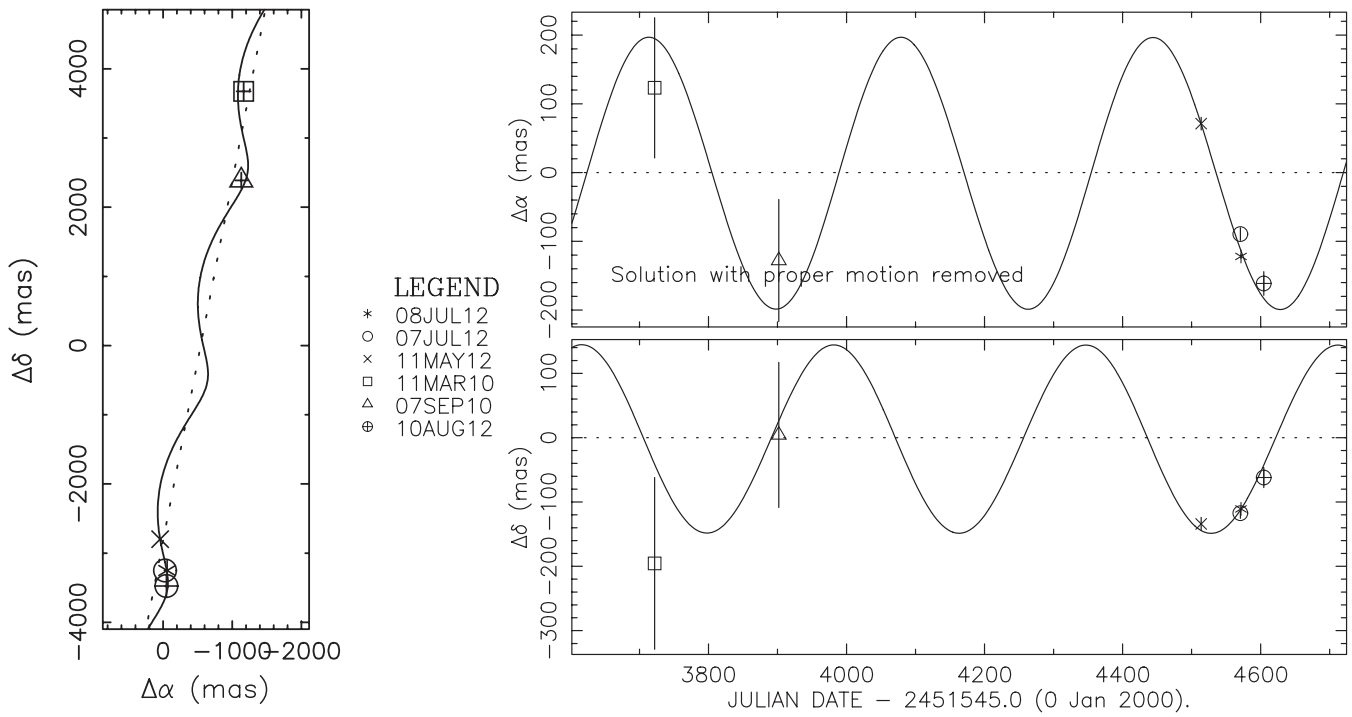

Figure 9. *WISE* and FourStar astrometry for W1639. Left panel shows actual motion on the sky with a proper motion and parallax solution superimposed. The *WISE* data are the two north most points (i.e., at the top of the panel). Right panels show the right ascension and declination solutions with the fitted proper motion removed for clarity. The *WISE* data are the two leftmost data points in each panel.

and astrometry for W1639 in the *All Sky* release arises from 11 epochs spread over a period of less than 2 days centered on 2010 March 11 (UT), while that in the *WISE 3 Band Cryo* release arises from 18 epochs centered on 2010 September 7 (UT). Because these data spans are short, we treat each observation as a single epoch obtained at the mean MJD of the observations that make up each catalog entry (as obtained from the relevant Single Exposure Source Tables). The result is a set of coordinates on the system defined by the 2MASS Point Source Catalog (Skrutskie et al. 2006). To enable a differential comparison with our FourStar images, these coordinates were tangent-projected about the *WISE All Sky* release position of W1639, scaled by the FourStar plate scale, and offset to place W1639 at the approximate location where it is actually observed in our FourStar images.

5.1. Results

The result is a set of observations in a FourStar pixel system, which we then subjected to standard differential astrometric processing (Tinney et al. 2003; Tinney 1996). A set of 20 reference stars was chosen to surround W1639 in the field of view. We required all 20 stars to be present in both *WISE* epochs and all FourStar epochs. The FourStar observations transfer on to the FourStar master frame with typical root-mean-square (rms) residuals of 3–5 mas. These astrometric precisions are for the reference stars, which in the FourStar data are typically much brighter than W1639 itself. Tests with background stars of similar magnitude to W1639 indicate that the FourStar astrometric precision for W1639 itself is ±8–10 mas, and these are the precisions that have been adopted in our astrometric solution.

In contrast, the *WISE* data have residuals with an rms of 100 mas. This is hardly surprising—*WISE* is a small telescope with 6″ resolution, so 0.″1 astrometric precision for this reference frame is itself remarkable. W1639 is quite bright in the *WISE* data, and the precision achieved for the reference stars is representative of that expected for W1639 itself. The 2 year time baseline delivered by *WISE* means that it provides critical astrometric information, in spite of this lower precision. The Magellan data constrain on the parallax motion, while the *WISE* data constrain the proper motion.

The resulting astrometric solution is shown in Figure 9. With only five independent epochs, and with two separate instruments coming into play, we consider this astrometry to be preliminary. In particular, the formal uncertainties do not reflect potential systematic differences between the two instruments' coordinate systems. Nonetheless, we see that W1639 has a *very* large proper motion (3069 ± 40 mas yr^{-1} at a P.A. = 169.1 ± 0.4 deg) which places it in the top 30 fastest moving stars in the solar neighborhood. The formal parallax solution is 200 ± 12 mas. With only five epochs in hand, this formal uncertainty will be an underestimate and the real uncertainty will be larger—we recommend considering this preliminary parallax good to ±20 mas until a FourStar-only parallax can be produced within the next 12 months. Parallactic motion has, nonetheless, been detected with high significance, and we expect this solution to rapidly improve over the next 12 months.

6. DISCUSSION

W1639 has a measured distance of 5.0 ± 0.5 pc. This places it comfortably inside the 8 pc nearby star sample and makes it about the 55th closest stellar system to the Sun (Kirkpatrick et al. 2012). The measured distance to W1639 implies an absolute magnitude in the J passband (using the correction from $J3$ to J adopted earlier) of $M_J = 22.14 \pm 0.22$. Figure 10 places this result in context with other late-T and Y dwarfs with measured parallaxes (spectral types are plotted as subtype+10 for Y dwarfs, and subtype+0 for T dwarfs). These

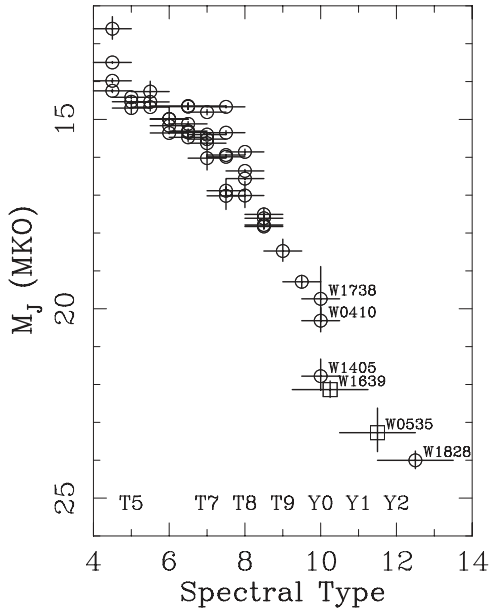

Figure 10. M_J absolute magnitude vs. spectral type for late-T and Y dwarfs. Objects plotted are those with extant parallaxes (as summarized in Table 6 of Kirkpatrick et al. 2012) as well as the W1639 data presented in this paper. *J* photometry is on the Mauna Kea Observatories system—objects from Kirkpatrick's table without MKO photometry available in the literature are not plotted. W1639 and WISE J053516.80−750024.9 have had *J*3 photometry converted to *J* as described in the text. Uncertainties on spectral types are plotted as ±0.5 subtypes except (a) where Kirkpatrick et al. only assign an upper limit spectral type, in which case the subtype is shifted by +0.5 and plotted with an uncertainty of ±1 subtypes (e.g., >Y1 is plotted as 11.5 ± 1); and (b) the spectral type is noted as uncertain, in which case it is plotted as ±1 subtype. W1639's Y0–Y0.5 type is plotted as 11.25 ± 1.

data suggest that W1639 has an absolute magnitude in the *J* passband at the lower end of that observed for Y0 brown dwarfs (and just slightly fainter than that for the Y0 brown dwarf WISEPC J140518.40+553421.5), but significantly brighter than the >Y1 brown dwarf WISE J053516.80−750024.9 (Kirkpatrick et al. 2012). This is in line with the spectra presented earlier, which suggest a Y0–Y0.5 spectral type.

Combining the distance and proper motion, W1639 has a significant tangential velocity ($V_{\rm tan}$) of 73 ± 8 km s^{-1}, and is among the fastest moving normal (i.e., non-subdwarf or non-low-surface-gravity) cool brown dwarfs yet observed (Faherty et al. 2009, 2012; Kirkpatrick et al. 2011). Faherty et al. (2012) derived the median $V_{\rm tan}$ and $\sigma_{\rm tan}$ values for the closely related T dwarf population to be 31 km s^{-1} and 20 km s^{-1} (respectively), suggesting that W1639 is kinematically deviant from brown dwarfs with ages typical of the field population (3–5 Gyr). While individual velocities cannot be used as an age indicator, general information can be obtained by comparing to the population of similar temperature objects. Faherty et al. (2009) found that the members of the population of high-$V_{\rm tan}$, low-temperature brown dwarfs show a correlation with being blue photometric outliers (and hence having either low-metallicity, high surface gravity, thin photospheric clouds, or a combination thereof), and can be regarded as being kinematically older than the field population. Using the measured distance, proper motion, and galactic coordinates ($l_{\rm II}$ = 321.2, $b_{\rm II}$ = −14.5), we have estimated likely values for the full space motion for W1639 (assuming a radial velocity in a range similar to the $V_{\rm tan}$ observed: −73, 0, and 73 mms) and find a range of *UVW* velocities which consistently place W1639 outside the "Eggen box" for young disk stars (<2 Gyr), indicating that this source is likely older than the field population (Eggen & Iben 1989).

While there are a limited number of Y dwarfs with distance measurements for comparison (Marsh et al. submitted; Beichman et al. submitted), Kirkpatrick et al. (2012) report $V_{\rm tan}$ values for a portion of newly discovered *WISE* brown dwarfs using photometric distance estimates for all sources. Two Y dwarfs, WISE 0410+1502 (Y0) and WISE 1405+5534 (Y0pec) also have significant tangential velocities ($V_{\rm tan}$ > 100 km s^{-1}). We note that this might be an indication that photometric distances are overestimated for these new sources. More Y dwarfs with distance measurements are needed to investigate whether the kinematics of the new low-temperature class of objects differs from that of the warmer brown dwarfs.

7. CONCLUSION

We have detected the near-infrared counterpart to the *WISE* mid-infrared source WISE J163940.83−684738.6. Spectroscopy indicates a spectral type of Y0–Y0.5, and this is consistent with the near-infrared-to-*WISE* $J3-W2$ color of W1639 which suggests it to be of type ≈Y1. W1639 is a bright, nearby Y dwarf—it is the brightest Y dwarf in the *W*2 passband in the *WISE* survey. It is likely to be a "hot button" target for future studies of the coolest brown dwarfs as its large proper motion moves it quickly away from the contaminating field star 2MASS J163940.83−684738.6 over the next 12 months.

These observations have shown, once again, that methane filters have significant utility in the follow-up of large surveys for cool brown dwarfs—the use of imaging permits the sort of differential analysis that can identify Y dwarfs even when they lie quite close to bright background stars, while the unique methane signature provides an unambiguous means of identifying very cool photospheres. Moreover, we have shown that methane filters placed in the near-infrared *J* band (as installed in FourStar) can be very powerful for observations of the coolest brown dwarfs. At very cold temperatures, the *J*-band methane signature is significant ($J2-J3 \lesssim -1.0$), and allows observers to take advantage of the much fainter sky in the *J* band—especially compared to that seen by more traditional *H*-band methane filters (Tinney et al. 2005).

C.G.T. gratefully acknowledges the support of ARC Australian Professorial Fellowship grant DP0774000. Australian access to the Magellan Telescopes was supported through the National Collaborative Research Infrastructure Strategy of the Australian Federal Government. Travel support for Magellan observing was provided by the Australian Astronomical Observatory.

This publication makes use of data products from the *Wide-field Infrared Survey Explorer*, which is a joint project of the University of California, Los Angeles, and the Jet Propulsion Laboratory/California Institute of Technology, funded by the National Aeronautics and Space Administration. This publication also makes use of data products from 2MASS, which is a joint project of the University of Massachusetts and the Infrared Processing and Analysis Center/California Institute of Technology, funded by the National Aeronautics and Space Administration and the National Science Foundation. This research has made extensive use of the NASA/IPAC Infrared Science Archive (IRSA), which is operated by the Jet Propulsion Laboratory, California Institute of Technology, under contract with the National Aeronautics and Space Administration.

And finally, this research has benefited from the M, L, and T dwarf compendium housed at DwarfArchives.org, whose server was funded by a NASA Small Research Grant, administered by the American Astronomical Society. We gratefully acknowledge the assistance of Phil Lucas and Ben Burningham who provided a digital copy of their UGPS 0722 spectrum.

Facilities: Magellan:Baade (FourStar, FIRE), *WISE*

REFERENCES

Bertin, E., & Arnouts, S. 1996, A&AS, 117, 393
Cavanagh, B., Jenness, T., Economou, F., & Currie, M. J. 2008, Astron. Nachr., 329, 295
Cushing, M. C., Kirkpatrick, J. D., Gelino, C. R., et al. 2011, ApJ, 743, 50
Draper, P. W., Allan, A., Berry, D. S., et al. 2005, in ASP Conf. Ser. 347, Astronomical Data Analysis Software and Systems XIV, ed. P. Shopbell, M. Britton, & R. Ebert (San Francisco, CA: ASP), 22
Eggen, O. J., & Iben, I., Jr. 1989, AJ, 97, 431
Faherty, J. K., Burgasser, A. J., Cruz, K. L., et al. 2009, AJ, 137, 1
Faherty, J. K., Burgasser, A. J., Walter, F. M., et al. 2012, ApJ, 752, 56
Kirkpatrick, J. D., Cushing, M. C., Gelino, C. R., et al. 2011, ApJS, 197, 19
Kirkpatrick, J. D., Gelino, C. R., Cushing, M. C., et al. 2012, ApJ, 753, 156
Lucas, P. W., Tinney, C. G., Burningham, B., et al. 2010, MNRAS, 408, L56
Persson, S. E., Barkhouser, R., Birk, C., et al. 2008, Proc. SPIE, 7014, 95
Saumon, D., Marley, M. S., Abel, M., Frommhold, L., & Freedman, R. S. 2012, ApJ, 750, 74
Simcoe, R. A., Burgasser, A. J., Bernstein, R. A., et al. 2008, Proc. SPIE, 7014, 70140U
Simcoe, R. A., Burgasser, A. J., Bochanski, J. J., et al. 2010, Proc. SPIE, 7735, 773514
Skrutskie, M. F., Cutri, R. M., Stiening, R., et al. 2006, AJ, 131, 1163
Stetson, P. B. 1987, PASP, 99, 191
Tinney, C. G. 1996, MNRAS, 281, 644
Tinney, C. G., Burgasser, A. J., & Kirkpatrick, J. D. 2003, AJ, 126, 975
Tinney, C. G., Burgasser, A. J., Kirkpatrick, J. D., & McElwain, M. W. 2005, AJ, 130, 2326
Wright, E. L., Eisenhardt, P. R. M., Mainzer, A. K., et al. 2010, AJ, 140, 1868